FEATURE ARTICLE

Reaction-Induced FT-IR Spectroscopic Studies of Biological Energy Conversion in Oxygenic Photosynthesis and Transport[§]

Sunyoung Kim[†] and Bridgette A. Barry*[,‡]

Department of Biochemistry, Virginia Polytechnic Institute and State University, Blacksburg, Virginia 24061-0308, and Department of Biochemistry, Molecular Biology, & Biophysics, University of Minnesota, St. Paul, Minnesota 55108-1022

Received: November 20, 2000; In Final Form: February 28, 2001

While membrane-associated proteins make up a substantial percentage of total cellular proteins, a much smaller fraction of known X-ray and NMR protein structures are derived from membrane proteins. Alternative approaches to understanding structure, function, and mechanism in membrane-associated enzymes are clearly needed. Vibrational FT-IR spectroscopy offers a method by which high-resolution structural and dynamic information can be obtained about this class of proteins. Reaction-induced FT-IR spectroscopy is an implementation of vibrational spectroscopy, in which the difference spectrum associated with a perturbative stimulus is recorded. This approach simplifies the spectrum and monitors the structural changes directly involved in the functional transition. In this article, we describe reaction-induced FT-IR studies of the photosynthetic and transport proteins, photosystem II, photosystem I, and lactose permease. In oxygenic plant photosynthesis, photosystem II and I convert light energy to chemical energy. In secondary active transport, the permease converts an electrochemical gradient into the energy required to move lactose into the cell. Reaction-induced FT-IR spectra acquired from these proteins can identify intermediates in the reaction mechanism. Vibrational bands in spectra acquired from photosystem II, photosystem I, and the permease are assigned by a combination of site-directed mutagenesis, isotopic labeling, and kinetic techniques. This article summarizes our recent progress in the study of photosynthetic and transport proteins with reaction-induced FT-IR spectroscopy.

Introduction

In respiration, photosynthesis, and transport, integral protein components of the membrane convert energy from one form into another. In photosynthesis, light energy is converted into chemical energy, in the form of a proton electrochemical gradient, $\Delta\mu_{H^+}$. In respiration, an electrochemical gradient is also generated, but the energy sources are low potential reductants, such as NADH, which are produced as a result of catabolic processes. In secondary active transport, an electrochemical gradient is converted into the energy required to move solutes against a concentration gradient. Respiration, photosynthesis, and transport are critical biological processes, and more information is needed about their detailed mechanism. An impediment has been the difficulty in acquiring high-resolution structural information about membrane-associated enzymes. Dynamic information about these proteins is even more difficult to acquire.

Vibrational FT-IR spectroscopy offers an approach with which high resolution structural information can be obtained about membrane proteins. The vibrational spectrum is an effective probe of enzymatic mechanism because the vibrational spectrum is altered by changes in conformation, configuration, protonation state, hydrogen bonding, polarity, and dielectric constant. Vibrational spectroscopy has the advantage that small sample sizes are employed, that time resolved experiments to obtain dynamic information are relatively easy to implement, and that perturbations of single amino acid residues can be detected, even in large complex proteins, given the high signal-to-noise ratios of contemporary FT-IR spectrometers {see, for example, ref 1}.

Reaction-induced FT-IR spectroscopy is an implementation of vibrational spectroscopy in which the difference spectrum associated with a perturbative stimulus is obtained. Infrared spectra are acquired of functional state A and of functional state B, and the data are subtracted to give the reaction-induced difference spectrum. This spectrum will reflect only the structural differences between state A and state B; using a stable infrared spectrometer, any vibrational bands that are not altered in frequency and intensity by the perturbation will cancel in the difference spectrum. This approach dramatically simplifies the spectrum and can provide information on the structural changes directly involved in the functional transition. Because changes in baseline can adversely affect such spectra, a single sample is modulated between the two functional states of interest. Even in a large complex membrane protein, with more than 8 subunits and a total molecular mass of more than 250 000

[†] Virginia Polytechnic Institute and State University.

[‡] University of Minnesota. Phone: 612-624-6732. Fax: 612-625-5780. E-mail: barry@biosci.cbs.umn.edu.

[§] Abbreviations: bchl, bacteriochlorophyll; chl, chlorophyll; cyt, cytochrome; EPR, electron paramagnetic resonance spectroscopy; EXAFS, extended X-ray absorption fine structure, FT-IR, Fourier transform infrared spectroscopy; P_{700}, primary electron donor of photosystem I; P_{680}, primary electron donor of photosystem II; PSI, photosystem I; PSII, photosystem II, XANES, X-ray absorption near edge spectroscopy.

10.1021/jp0042516 CCC: $20.00
Published on Web 04/13/2001

daltons, protonation and redox changes involving single amino acid residues can be detected.[1,2] Kinetic experiments can also be implemented by rapid scan or step scan approaches.

Reaction-induced, or light-minus-dark, FT-IR spectroscopy was applied in studies of the membrane protein, bacteriorhodopsin, approximately 20 years ago.[3,4] Bacteriorhodopsin is an approximately 26 000 dalton protein that contains a retinal Schiff base chromophore.[5] Upon photoexcitation, the retinal chromophore absorbs light and isomerizes from the all-trans to 13-cis configuration.[6−8] This isomerization drives protein structural changes and pK_a shifts in amino acid side chains. A sequence of proton-transfer reactions leads to transmembrane proton transfer.[9−12] Because intermediates in the isomerization and proton-transfer reactions can be trapped by alteration of sample conditions, such as temperature, reaction-induced FT-IR spectroscopy was important in deciphering the mechanism of proton transfer in this enzyme {reviewed in ref 13}.

Reaction-induced, light-minus-dark, FT-IR spectroscopy has been used to study other light-absorbing proteins, including, for example, sensory rhodopsin,[14] halorhodopsin,[15] visual rhodopsins,[16] phytochrome,[17] and the reaction center from purple, nonsulfur bacteria[18] and from heliobacteria,[19] among others. Electrochemical methods have also been employed to obtain the difference FT-IR spectrum associated with redox changes in enzymes {see ref 20 for an example}.

Although the reaction-induced approach simplifies the biological spectrum, assignment of these difference spectra is still a challenge. Use of a combination of approaches is helpful. In our work, this combination has included the development of methods to incorporate stable isotopes into amino acid residues and prosthetic groups, the generation of site-directed mutations, in which substitutions at individual amino acids are introduced genetically, and the use of kinetic comparison to other spectroscopic methods of monitoring mechanism, such as EPR spectroscopy. In practice, this assignment method means that prokaryotic sources of the membrane proteins are preferred. We have applied this approach in studies of the photosynthetic enzymes, PSI and PSII, which catalyze oxygenic photosynthesis.[1,2,21−36]

Recently, we have also successfully applied reaction-induced FT-IR spectroscopy to a transport protein, the lactose permease, which is not directly photoactivatable.[37] To monitor the effect of an electrochemical gradient on the permease, the protein was incorporated into a liposome containing bacteriorhodopsin, which acted as the light-inducible trigger for the electrochemical gradient. This approach will ultimately give new information about membrane transport.

In this article, we summarize our recent progress in the study of photosynthetic and transport proteins with reaction-induced FT-IR spectroscopy. In photosynthesis, a variety of topics will be introduced. In some of these studies, experiments have advanced to the point that new functional information is available. In others, experiments are at an earlier stage and have led to the identification and assignment of vibrational bands, which will provide the basis for future functional studies. In transport, reaction-induced FT-IR studies are in the beginning stages, but the discussion here will illustrate the possibilities of the technique, when applied to proteins that are not directly photoactivatable.

Photosynthesis

Photosynthesis in plants, green algae, and cyanobacteria involves the concerted action of two photosystems, PSI and PSII.

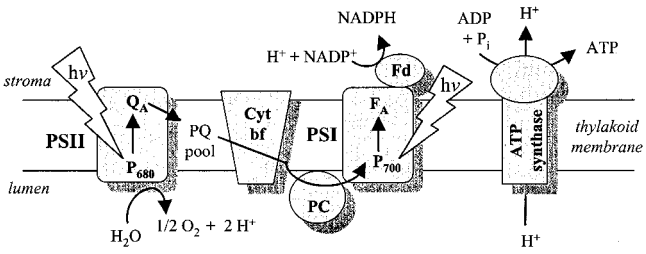

Figure 1. Diagram of the photosynthetic electron-transfer chain.

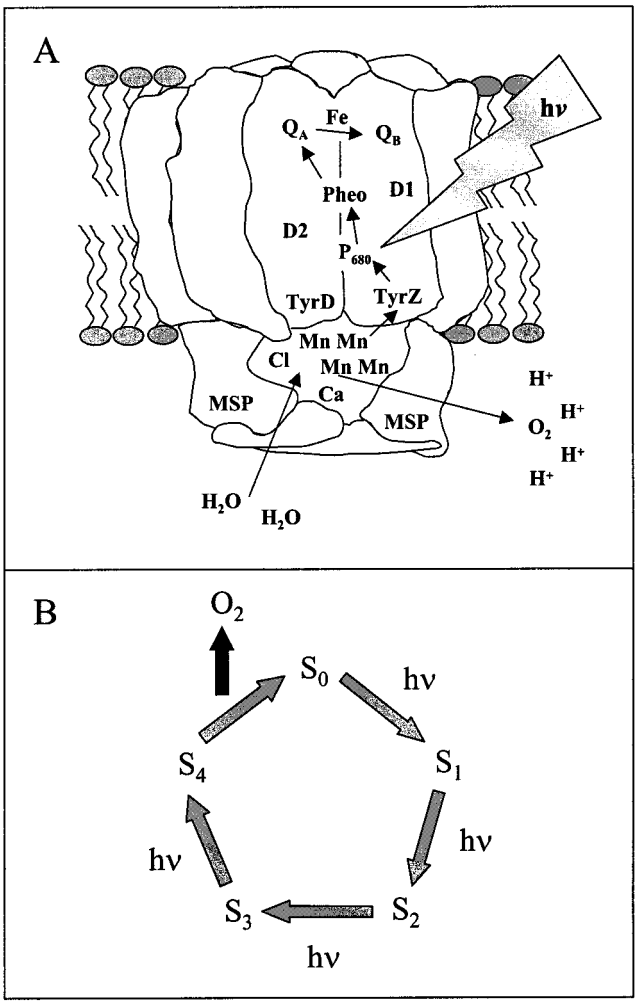

Figure 2. Cartoon model of PSII structure, based on a recently reported structural model[92] (A) and mechanism for photosynthetic water oxidation[43] (B).

These photosystems are reaction centers that absorb light and generate a charge separation. Together, PSI and PSII move electrons from water to $NADP^+$. A proton gradient is generated by combined electron and proton-transfer reactions in PSII and the cytochrome bf complex, which acts as an intermediary in the electron-transfer reactions (Figure 1). The mechanism of the PSII and PSI reactions can be addressed with reaction-induced FT-IR spectroscopy. We have performed an extensive set of studies on PSII, including an investigation of the water splitting reactions, of redox active tyrosines, of extrinsic subunit assembly and function, of site-directed mutants, and of a quinone acceptor. Recently, we have extended our work to address structure and function in the PSI reaction center.

A. Photosystem II. PSII carries out the light-driven oxidation of water and reduction of plastoquinone (Figure 2A). Electron transfer is initiated when the primary chl donor, P_{680}, absorbs

light. Subsequent, sequential electron-transfer reactions lead to the production of a chl cation radical, P_{680}^+, and reduction of pheophytin, a single electron accepting plastoquinone, Q_A, and of Q_B, a two electron acceptor {reviewed in ref 38}. P_{680}^+ is very unstable and readily generates other oxidized species.[39] One of these oxidized species, tyrosine Z,[40] is an intermediary in electron-transfer reactions involving P_{680} and the catalytic site for water oxidation, which contains four manganese atoms.[41] Another redox active tyrosine, D, is also oxidized via P_{680}^+ and is in redox equilibrium with the manganese cluster.[42] The catalytic site of water oxidation cycles among five oxidation states, called the S_i states, where *i* refers to the number of oxidizing equivalents stored at the active site.[43] Each S state advancement is driven by one light-driven charge separation in the reaction center (Figure 2B). The oxidation of one molecule of water is accompanied by reduction of two molecules of plastoquinone. An extrinsic subunit, called the manganese stabilizing protein (MSP, Figure 2A), is required for optimal efficiency of oxygen evolution.[44]

In this article, we present examples of the application of reaction-induced FT-IR spectroscopy to electron and proton-transfer reactions in PSII. The order of presentation will begin with events on the stromal side of the membrane (Figure 2A), i.e., the light-induced reduction of plastoquinone, where we have identified the vibrational contributions from plastoquinone by isotopic labeling. The article will then go on to discuss events on the lumenal side of the membrane (Figure 2A), where functional information has been obtained concerning redox active tyrosines. We also describe our FT-IR studies of the S state transitions and the assembly and function of the subunit, MSP, in oxygen production.

Vibrational Spectrum of Q_A^- in PSII. Quinone acceptor molecules are found in Type II reaction centers, which include both PSII[38] and the bacterial reaction center from purple, nonsulfur bacteria.[45] Each reaction center contains two quinones, which can have identical molecular structures (Figure 2A). However, the protein binding site selects quinone redox function. The quinone known as Q_A acts only as a single electron acceptor, and the quinone known as Q_B sequentially accepts two electrons and two protons.

Vibrational spectroscopy can be employed to obtain information about how this specificity in function is imposed on the primary and secondary quinone acceptors. This approach has been used to study the photoinduced reduction of the quinone acceptors in bacterial reaction centers. These reaction centers do not contain a water splitting complex and lack the organic donor side radicals found in PSII. In these reaction centers, Q_A can be removed and reconstituted,[46] and this reconstitution procedure led to the use of isotopic labeling to identify vibrational bands from the quinones. Application of FT-IR and Raman spectroscopy to isotopically labeled reaction centers has given insights into the role of amino acids in the environments of the quinone acceptors.[18,47]

However, to our knowledge, there are no methods to remove and reconstitute Q_A that do not lead to inactivation of the PSII enzyme. Also, organic radicals from the donor side are readily produced because of the high redox potential of P_{680}, and contributions from these species, i.e., tyrosyl radicals, complicate the vibrational spectrum.[23] Therefore, the origin of bands from the quinones has been controversial {see discussion in ref 32}. The original assignment of bands to Q_A^- on the basis of group frequency assignments[48] was questioned,[23] because the possibility of overlapping contributions from donor side species was not considered in the original work.

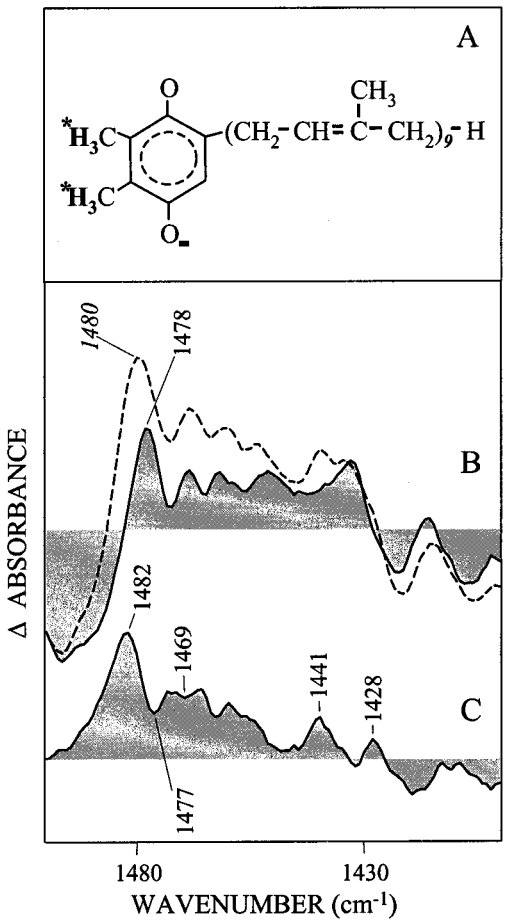

Figure 3. Deuteration of plastoquinone from methionine (A) and effects of such deuteration on the spectrum of Q_A^--minus-Q_A (B). In (B), the control spectrum is shown as the dashed line; the spectrum obtained after $^2H_3$ labeling is shown as the solid line. The isotope-edited spectrum, control-minus-labeled, is also presented (C). Spectral conditions are reported in ref 32. The asterisks show the sites of labeling (A).

TABLE 1: Normal Mode Assignments and Experimentally Measured Vibrational Frequencies (cm^{-1})[32]

neutral quinone	decyl-PQ	PQ-9	Q_A
CO antisymmetric stretch	1653	1652	1659
ring CC/CO symmetric stretch	1633	1633	1631[a]
ring CC antisymmetric stretch	1617	1618	1611[a]
semiquinone anion radical	**decyl-PQ$^-$**	**PQ-9$^-$**	**Q_A^-**
ring CC antisymmetric stretch	1474	1471	1482
CO antisymmetric stretch	1454	1452	1469
ring CH bend/CC stretch	1418	1409	NA

[a] Tentative assignment.

To use FT-IR spectroscopy as an effective probe of quinone structure and function, identification of bands must be performed through isotopic labeling of plastoquinone. In situ isotopic labeling of plastoquinone, in an organism from which PSII can be isolated, was achieved recently.[32,35] Plastoquinone was methyl deuterated (Figure 3A) by culturing cyanobacteria in the presence of deuterated methionine.[42] Selection was applied in order to isolate a methionine-tolerant strain that would take up this amino acid. Labeling of other amino acids, including tyrosine, appeared to be negligible when this approach was employed.[35] Density functional calculations identified the expected isotope shifts upon methyl deuteration for plastoquinone and its semiquinone anion radical.[32] The spectrum associated with the reduction of plastoquinone was obtained in

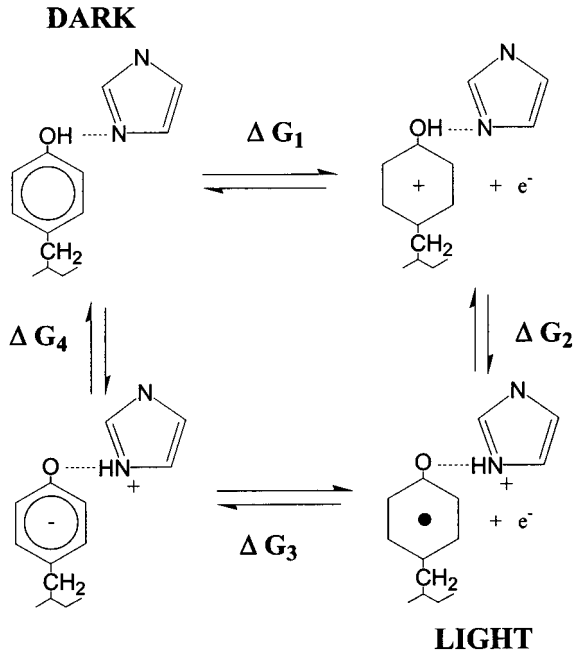

Figure 4. Thermodynamic box illustrating the linkage between tyrosine oxidation and histidine protonation in PSII. A neutral tyrosyl radical is depicted at the lower right (light).

ethanol.[32] Comparison of calculated and in vitro data with spectra acquired from PSII was used to derive a preliminary set of normal coordinate assignments for Q_A and Q_A^- (Table 1). These studies showed that Q_A^- contributions to the PSII spectrum are expected at approximately 1480 cm^{-1} (CC stretch) and 1469 cm^{-1} (CO stretch). In PSII, vibrational bands are observed at those frequencies. Confirming the calculations, both those bands exhibited downshifts upon methyl deuteration (Figure 3B,C). The fact that these contributions are overlapping with spectral contributions from the PSII tyrosyl radicals accounts for the confusion over these assignments in the literature {reviewed in refs 30 and 35}. Our Q_A^- assignments support the conclusions of a recent kinetic study of Q_A^- decay[49] and the initial suggestion that Q_A^- contributes to the spectrum in the 1490−1470 cm^{-1} region.[48] With this basis, vibrational techniques can now be applied to the structure/function of Q_A^- in PSII. Q_B^- assignments are in progress.

Vibrational Spectra of Tyrosyl Radicals in PSII. Two redox-active tyrosines, termed tyrosine Z and tyrosine D, are oxidized by the primary electron donor, P_{680}^+, to form neutral, deprotonated tyrosyl radicals, D• and Z• (Figure 4).[39,42] Tyrosines Z and D are in symmetric positions within the core of PSII;[50] site-directed mutagenesis[51−55] identified tyrosines Z and D as residues Y161 in the D1 polypeptide and Y160 in the D2 polypeptide, respectively. Despite their symmetric locations in the D1 and D2 polypeptides, which have a high degree of sequence similarity, D and Z have different kinetic and energetic properties. Tyrosine Z is required for light-induced oxygen evolution,[52,54−56] whereas tyrosine D is not required.[51,53,57] However, it has been suggested that tyrosine D may be involved in the stabilization of the manganese cluster in the dark.[58] Tyrosine Z is more rapidly oxidized when compared to tyrosine D and is the intermediate electron carrier between P_{680}^+ and the manganese cluster. Because of its short lifetime, tyrosine Z is the more difficult radical species to study. The neutral tyrosyl Z• and D• radicals are reduced by the manganese cluster with a $t_{1/2}$ of microseconds−milliseconds[59] and minutes−hour,[60] respectively. The oxidation potentials of D and Z are estimated to be 760 mV[61] and 1 V.[54] These alterations in redox potential and radical lifetime must reflect protein environmental influences.

Because D• and Z• are neutral tyrosyl radicals, oxidation of D and Z is necessarily coupled to proton transfer. As illustrated in Figure 4, the pK_a of the proton-accepting group is then thermodynamically linked to the electron-transfer reactions resulting in the oxidation of the redox active tyrosine. There are two possible pathways between the dark and light states. On one path (Figure 4, 1+2), oxidation of tyrosine, yielding a tyrosine cation radical, precedes proton transfer. On the other (Figure 4, 4+3), deprotonation of tyrosine precedes electron transfer. This formalism suggests that the pK_a of the proton acceptor can alter the redox potential of redox active tyrosines. In turn, such energetic changes could alter electron-transfer rates.[62]

Previous magnetic resonance experiments demonstrated that His189 in the D2 polypeptide is the hydrogen bond partner for D• and suggested that His189 functions as the proton-accepting group.[63,64] The immediate proton acceptor for tyrosine Z has been attributed to His190 in the D1 polypeptide in some studies[65,66] but not in others.[22,67,68] Thus, the hydrogen bonding status of tyrosine Z• is still unclear, but the radical may be hydrogen bonded to water.[22,68,69,70] It is important to point out that preparations employed in these tyrosine Z• studies lack manganese and extrinsic polypeptides, to slow the rate of Z• reduction. It is possible that this alteration could cause additional changes in the structure of PSII.

Difference FT-IR spectroscopy provides a direct method to identify the proton-accepting group, because the protonation spectrum of the acceptor should contribute to the difference spectrum. The hypothesis that the oxidation of tyrosine D is coupled to proton transfer was tested through the combination of site-directed mutagenesis, EPR, and FT-IR spectroscopy.[1] His189D2 was modified to leucine (HL189D2) by mutagenesis of the D2 gene. Imidazole rescue[71−76] was then used to test whether imidazole could substitute functionally for His189 (Figure 4).

To directly observe the D• radical, we first employed EPR spectroscopy.[1] In controls, D• was produced and decayed with a halftime of approximately 15 min.[1] Mutation of His189D2 to leucine resulted in a decrease in tyrosyl D• radical yield and decay rate. Incubation of HL189D2 PSII with imidazole increased the yield and accelerated the rate of tyrosyl D• decay.[1] These data suggested that the reconstituted imidazole is able to functionally replace His189.

To directly observe the proton acceptor for tyrosine D, difference FT-IR techniques were next employed. If the imidazole ring is reversibly protonated and deprotonated upon alteration of the redox state of tyrosine, the vibrational spectrum associated with the protonation of imidazole will be observed, as well as the spectrum associated with D oxidation. By exploiting differences in the decay rate of the oxidized tyrosyl radicals, the oxidation spectra of D and Z can be distinguished and acquired on the same sample.[2,21,22,26,28] Using this approach, a band at 1478 cm^{-1} was assigned to ν(CO) of Z•; at pH 7.5, a band at 1477 cm^{-1} was assigned to ν(CO) of D• (Figure 5A).[2,26,28,35,77] The frequency and amplitude of the CO stretch of D• were sensitive to changes in buffer and pH.[2,27,28] The 1478/1477 cm^{-1} assignments were based on isotopic labeling of tyrosine, site-directed mutagenesis, the use of inhibitors, and kinetic analysis.[2,26−28,30,35] Mutagenesis of His189 to leucine was shown to decrease the intensity of the 1477 cm^{-1} band (Figure 5B); introduction of imidazole restored intensity (Figure 5C).

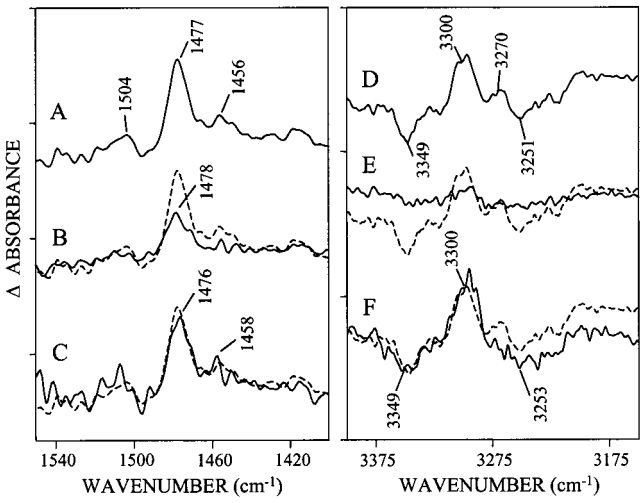

Figure 5. Tyrosine D•-minus-D spectrum obtained from wildtype (A and D), the HL189D2 mutant (B and E), and the HL189D2 mutant plus imidazole (C and F). Spectrum A is repeated as the dotted line in (B) and (C). Spectrum D is repeated as the dotted line in (E) and (F). Spectral conditions are reported in ref 1.

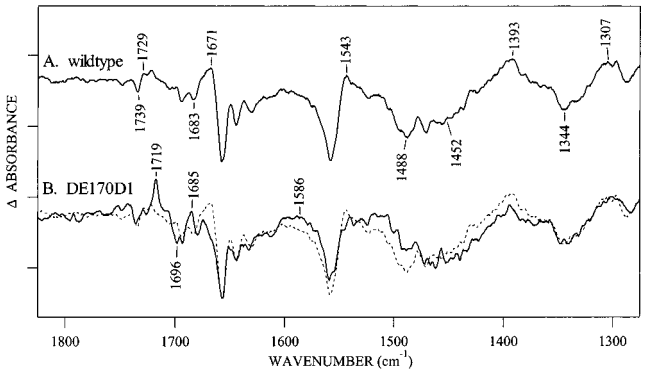

Figure 6. Light-minus-dark FT-IR spectrum associated with $S_2Q_A^-$-minus-S_1Q_A at 200 K in wild-type PSII (A), and PSII isolated from the DE170D1 mutant (B). The spectrum shown in (A) is repeated in (B) as the dotted line, to facilitate comparison. The $S_2Q_A^-$-minus-S_1Q_A spectra in both wild-type[24,25,29] and DE170D1[33] PSII were dramatically altered by removal of the manganese cluster, as expected. Spectral conditions are reported in ref 33.

Bands in the 3350−3250 cm^{-1} region of the D•-minus-D spectrum (Figure 5D) were assigned to N−H stretching vibrations arising from His189D2. This assignment was based on global ^{15}N labeling and deuterium exchange, as well as site-directed mutagenesis.[1] Mutation of His189D2 to leucine eliminated spectral features in the 3350−3250 cm^{-1} region (Figure 5E), whereas addition of imidazole to HL189D2 resulted in spectral features that were similar, but not identical, to those in the control spectrum (Figure 5F).

Taken together, these studies indicate that His189D2 contributes to the FT-IR spectrum associated with the oxidation of tyrosine D. These spectral contributions can be detected because histidine undergoes a reversible structural change (Figure 4) that is coupled to the electron-transfer reaction. Based on comparison with the protonation spectrum of imidazole in vitro,[80−86] and our own model compound data (not shown), this reversible structural change is a protonation. Therefore, His189 in the D2 polypeptide is the proton acceptor for tyrosine D, and imidazole can chemically rescue a mutation at this residue. Furthermore, the study described here gave the first direct evidence that proton transfer (see Figure 4) is a requirement for efficient electron transfer involving tyrosine D. Studies of other tyrosyl radicals, including tyrosine Z, will eventually provide comparative information with which to understand the factors that control the function of these redox active species in PSII and in other enzymes.[39]

Reaction-Induced FT-IR Studies of the S State Transitions in the PSII Oxygen-Evolving Complex. Reaction-induced FT-IR studies can be used to probe the mechanism of the water splitting reactions. FT-IR spectroscopy is complementary to the use of other techniques, such as EPR spectroscopy[38] and can detect changes in manganese ligation, manganese oxidation state, protonation changes, perturbations of bound water, and formation of the oxygen−oxygen bond. A key advantage is the relatively small sample size required for the FT-IR measurements as compared to EPR and X-ray studies, because small sample size facilitates the use of expensive or precious samples. Also, detection and study of each S state transition requires sequential laser flashes and good synchronization; therefore, small sample size, when the sample is an absorber, is an important benefit.

In FT-IR spectroscopy, all structural changes in the reaction center are reflected in the spectrum. For example, as laser flashes are used to advance through the S state cycle, electron-transfer reactions are also occurring on the acceptor side of the reaction center. Therefore, many control experiments, using complementary techniques such as EPR spectroscopy, are necessary in order to verify the redox state of the sample.

As a first step in this FT-IR investigation of the water oxidizing complex, this group employed cryogenic conditions.[24,25,29] Data acquired by continuous illumination at 200 K are presented in Figure 6A. Appropriate control experiments were performed to verify that charge separation had occurred.[24,25,29,31,33] The $S_2Q_A^-$-minus-S_1Q_A FT-IR spectrum (Figure 6A) exhibited broad bands between 1500 and 1200 cm^{-1}, which have been assigned to amino acid residues in the environment of the manganese cluster.[24,25,29,31,33] These amino acid residues must be perturbed by the photooxidation of manganese. This conclusion is supported by the mutagenesis study described below. Our group observes an apparent temperature dependence in the FT-IR spectrum.[24,25,31] Data obtained at higher temperatures resemble spectra obtained by other groups and attributed to $S_2Q_A^-$-minus-S_1Q_A.[87−89] Possible origins of this apparent dependence on temperature have been discussed.[31,90] We are now using flash sequences to synchronize and advance through the S state cycle at higher temperatures, where oxygen can be produced.

Carboxylate Ligation Shifts at the Active Site for Water Oxidation. The heterodimeric core of PSII is made up of two polypeptides, called D1 and D2 (Figure 2A). These subunits bind many of the cofactors needed for electron transfer.[91,92] Each polypeptide is predicted to have five transmembrane α helical domains.[93] The lumenal loops of D1 and D2 have been identified as potential sites of ligation for the manganese atoms {reviewed in ref 94}.

Aspartate 170 in the D1 polypeptide is such a potential ligand. It has been shown that site-directed mutations at aspartate 170 alter the properties of the manganese cluster.[95,96] Out of eleven introduced mutations at this site, nine abolished the ability of the mutant cyanobacterial cells to grow photosynthetically and dramatically reduced oxygen evolution activity. The aspartate to glutamate mutation did not abolish oxygen evolution, but the mutation resulted in a 2−3-fold decrease in specific activity. Spectroscopic evidence indicated that an active manganese cluster was assembled in this mutant.[95,96]

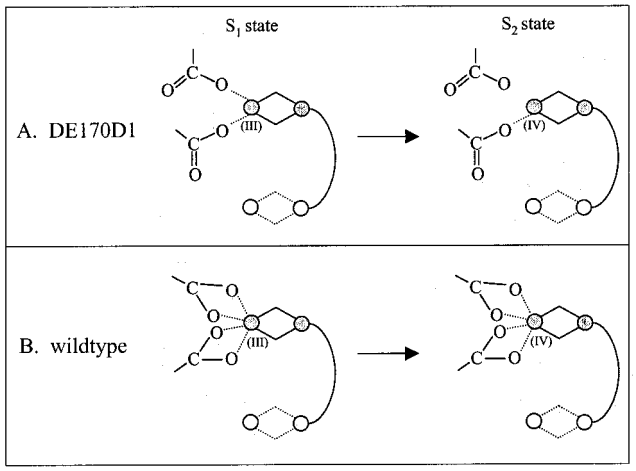

Figure 7. Speculative model of mutation-induced carboxylate shifts at the PSII manganese cluster. Figure reprinted with permission from *J. Biol.Chem.*[33]

We investigated the properties of the aspartate to glutamate mutant (DE170) with FT-IR and EPR spectroscopy.[33] Our FT-IR experiments showed perturbations in the 200 K $S_2Q_A^-$-minus-S_1Q_A spectrum, consistent with a change in carboxylate ligation in the DE170 mutant (Figure 6B). This change in ligation may be from bridging/bidentate carboxylate ligation in the wildtype to unidentate carboxylate ligation in the mutant (Figure 7). These observations are consistent with carboxylate shifts at the active site of PSII. We postulate that these shifts are induced by the change in side chain volume when glutamate is substituted for aspartate. Functionally important carboxylate shifts are known to occur at the active sites of other metalloenzymes and to be associated with redox changes at the active site.[97,98] In the future, this possibility can be explored by using difference FT-IR spectroscopy to study PSII water oxidation at higher temperatures.

Assembly and Possible Role of an Extrinsic Subunit in Water Oxidation. PSII contains an extrinsic subunit (Figure 2A), called the manganese stabilizing protein (MSP), which plays a role in promoting the efficiency of the water splitting reactions and the stability of the manganese cluster {see ref 99 and references therein}. As an extrinsic subunit, MSP can be removed from PSII (Figure 8A) by treatment with urea or calcium chloride and then studied in solution.[100−103] The specific activity of oxygen evolution drops when MSP is removed from the PSII reaction center. MSP can then be reconstituted (Figure 8B), and oxygen evolution rates, similar to the control, are regained.[104] To understand the mechanism by which MSP alters the rate of oxygen evolution and by which MSP is assembled in vitro, we have uniformly ^{13}C-labeled MSP by growth of an expressing *Escherichia coli* strain on ^{13}C-glucose.[31,99] FT-IR spectroscopy is sensitive to isotopic composition. Therefore, uniform labeling of MSP allows structural changes in this subunit to be detected and monitored, even when MSP is bound to the PSII reaction center (Figure 8B). Little is known about the assembly and function of extrinsic subunits in complex membrane proteins, and PSII provides a model system in which to investigate these questions.

FT-IR spectroscopy can be used to determine the secondary structure of proteins.[105,106] The amide I (C═O) stretching frequency has been shown to be correlated with secondary structure.[107,108] Because a protein amide I band is a superposition of broad bands arising from each secondary structural element, the amide I line shape must be analyzed to identify inflection points {see Figure 8 for examples}. The band is then fit with

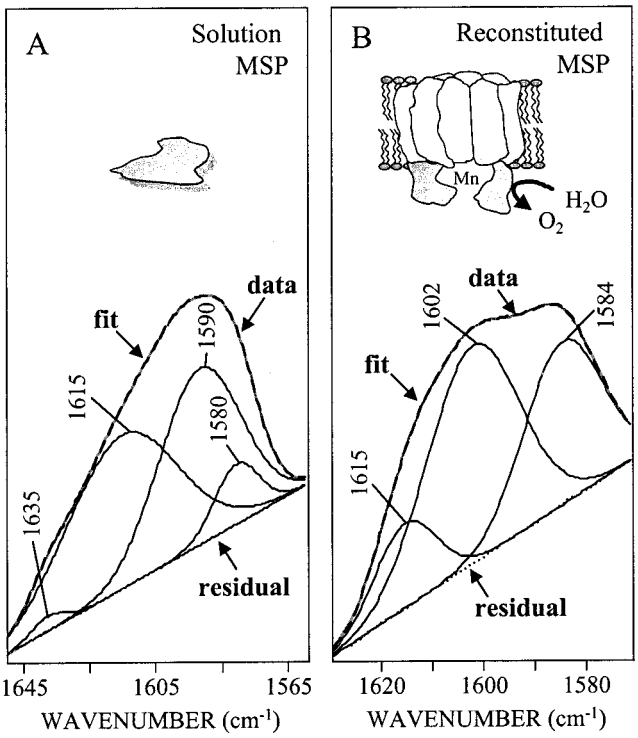

Figure 8. Gaussian fits to the FT-IR amide I line shape derived from ^{13}C-labeled MSP in solution (A) and after reconstitution to PSII (B). To generate (B), infrared spectra were subtracted, using an internal standard, to eliminate the background from ^{12}C PSII. Spectral conditions and data analysis parameters are reported in ref 99.

Gaussian lines to determine the percentage of the total structure corresponding to each secondary structural element (Figure 8). Certain secondary structural elements (for example, loops and helices) have overlapping frequency ranges {reviewed in refs 105 and 106}. This FT-IR approach was employed to determine the secondary structure of MSP in solution.[99,109] MSP was released from the PSII reaction center either with urea or calcium chloride, purified, and studied in ^2H_2O solutions.[99] ^2H_2O buffers were employed because ^1H_2O has an O−H bending mode that obscures the amide I C═O band. In these experiments, the amide I line shape of MSP varied dramatically. In one urea-released sample, the result was consistent with the following secondary structural elements: α helix or loops (∼70%), β sheet (∼20%), and random unassigned structure (∼10%). In a calcium chloride-released sample, the result was consistent with the following secondary structural elements: α helix or loops (∼75%) and turns (∼25%). When MSP was isolated from *E. coli*, the analysis was consistent with the following secondary structural elements: α helix or loops (∼40%), β sheet (∼45%), random structure (∼15%). These results suggest that MSP can sample a variety of conformational states in solution.[110] However, all these preparations bind to PSII and restore oxygen evolution activity.[99] On the basis of these and other measurements, it was proposed that MSP is natively unfolded in solution.[110]

Given that the structure of MSP is variable in solution, its secondary structure when bound to PSII became the next question. This issue was investigated using an isotope-editing approach in which MSP was uniformly labeled with ^{13}C.[99] Using this globally ^{13}C-labeled material, the amide I band of MSP can be detected even when MSP is bound to the PSII reaction center. This is possible, because ^{13}C-labeling downshifts the MSP amide I band by approximately 50 cm^{-1}. For data analysis, an internal standard was employed to subtract the spectrum of

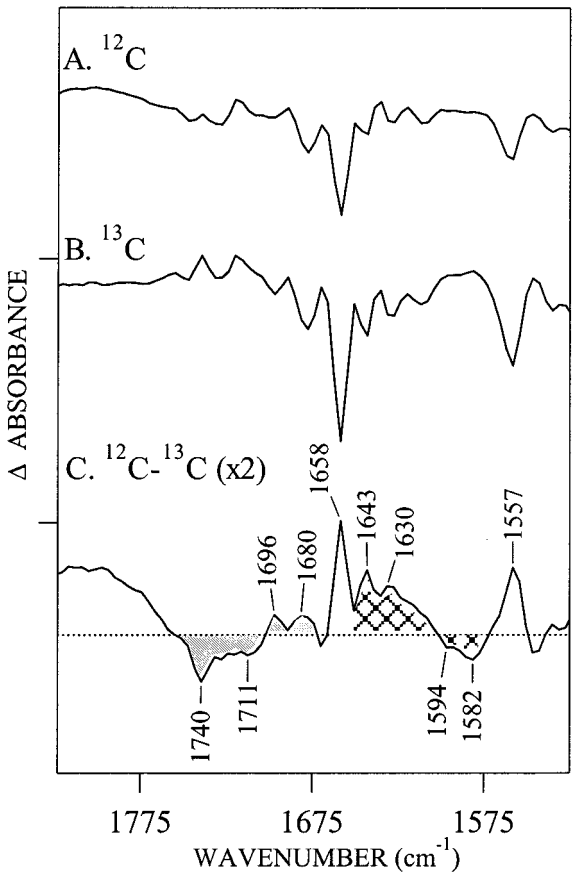

Figure 9. Light-minus-dark FT-IR spectrum associated with $S_2Q_A^-$-minus-S_1Q_A at 200 K. In (A), the spectrum was obtained from a PSII sample containing ^{12}C-MSP. In (B), the spectrum was obtained from a PSII sample containing ^{13}C-MSP. The double difference spectrum, which is isotope-edited, is shown in (C). Vibrational bands assigned to the C═O stretch of carboxylic acids in MSP have solid fill. Vibrational bands assigned to the asymmetric OCO stretch of carboxylates in MSP have hatched fill. Spectral conditions are reported in ref 31.

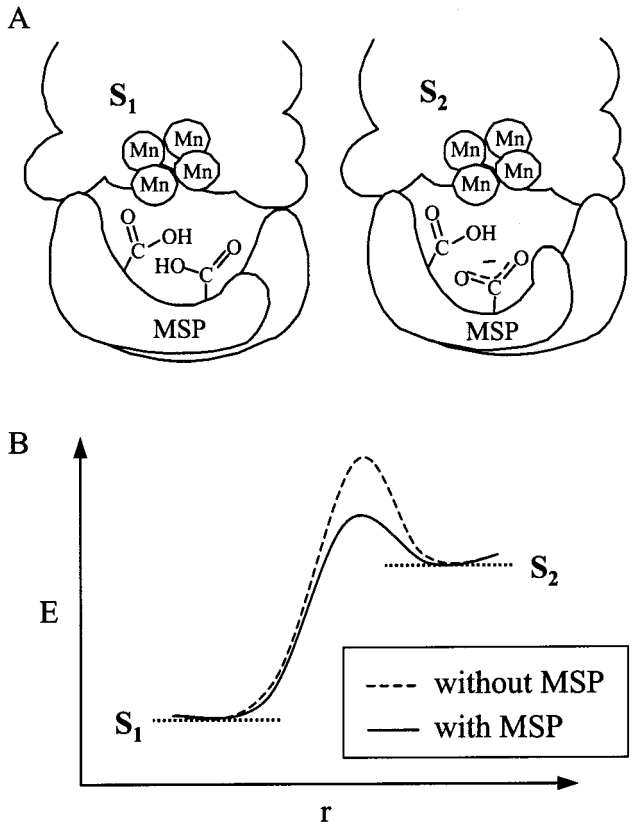

Figure 10. Deprotonation of a carboxylic acid residue on MSP during the S_1 to S_2 transition (A) and illustration of the possible effects of deprotonation on the rate of the S_1 to S_2 transition (B).

the control (^{12}C-MSP rebound PSII) from the spectrum of the ^{13}C-MSP sample. Such a difference spectrum, obtained in ^2H_2O buffer, is shown in Figure 8B. When the same ^{13}C-MSP protein sample was compared before (Figure 8A) and after (Figure 8B) reconstitution, a 30−40% change in secondary structure was observed (compare fits to Figure 8A,B). The results were consistent with an increase in β sheet structure at the expense of randomized structure. These results also suggested that MSP interacts with PSII through β strands and that binding induces folding of MSP.[99] Flexibility in the structure of MSP in solution may be important in promoting its interaction with its PSII binding site[110] and may be important in its function during oxygen evolution.[31]

^{13}C-labeled MSP and isotope editing were also used to investigate the role of MSP during oxygen evolution, specifically during the S_1 to S_2 transition.[31] Our hypothesis was that conformational changes on MSP might accompany the S state transitions. As a first step toward testing this idea, the light-minus-dark $S_2Q_A^-$-minus-S_1Q_A spectrum was acquired at 200 K. PSII samples were employed to which either ^{12}C-MSP (Figure 9A) or ^{13}C-MSP (Figure 9B) had been reconstituted. Spectra were corrected for any small differences in path length and concentration and were then subtracted to give an isotope-edited spectrum that reflects only changes in MSP (Figure 9C). This spectrum exhibits negative vibrational bands at 1740 and 1711 cm^{-1} and positive bands at 1696 and 1680 cm^{-1} that have been assigned to the ^{12}C═O and ^{13}C═O stretches of carboxylic acids, respectively (Figure 9C, solid fill). Positive bands at 1643 and 1630 cm^{-1} and negative bands at 1594 and 1582 cm^{-1} were assigned to the asymmetric OCO stretching vibration of ^{12}C and ^{13}C carboxylates, respectively (Figure 9C, hatched fill). Therefore, these data are consistent with deprotonation of one or more glutamic and aspartic acid residue(s) in MSP (Figure 10A) during the S_1 to S_2 transition.[31] Evidence for small secondary structural changes on MSP was also acquired, because spectral contributions in the amide I and II regions were observed (see bands at 1658 and 1557 cm^{-1}, Figure 9C). These structural changes on MSP may be driven by the photooxidation of manganese during the S_1 to S_2 transition.[31] The functional role of MSP may be to generate one or more negative charges in the environment of the manganese cluster. Generation of this negative charge may stabilize a charged transition state (Figure 10B) and account for the kinetic effects of MSP reconstitution on the S state transitions, which were observed to be an acceleration of both forward and reverse reactions.[111−113] Investigation of conformational changes in MSP during other S state transitions is in progress.

B. Photosystem I. We have recently begun to investigate the factors that control the midpoint potential of the primary chl donor in PSII and PSI. PSII and PSI have primary donors composed of a dimer of chl a[92] and a dimer of chl a and its epimer, chl a′ {Prof. H. T. Witt, personal communication}, respectively. The oxidation potentials of the primary donors differ by approximately 600 mV {reviewed in ref 114}. To contribute to an understanding of this energetic difference, which must be imposed by the protein environment,[115] we have begun a study using vibrational spectroscopy. The reaction-induced FT-IR spectrum associated with primary donor oxidation will be obtained, and chl vibrational bands will be identified by

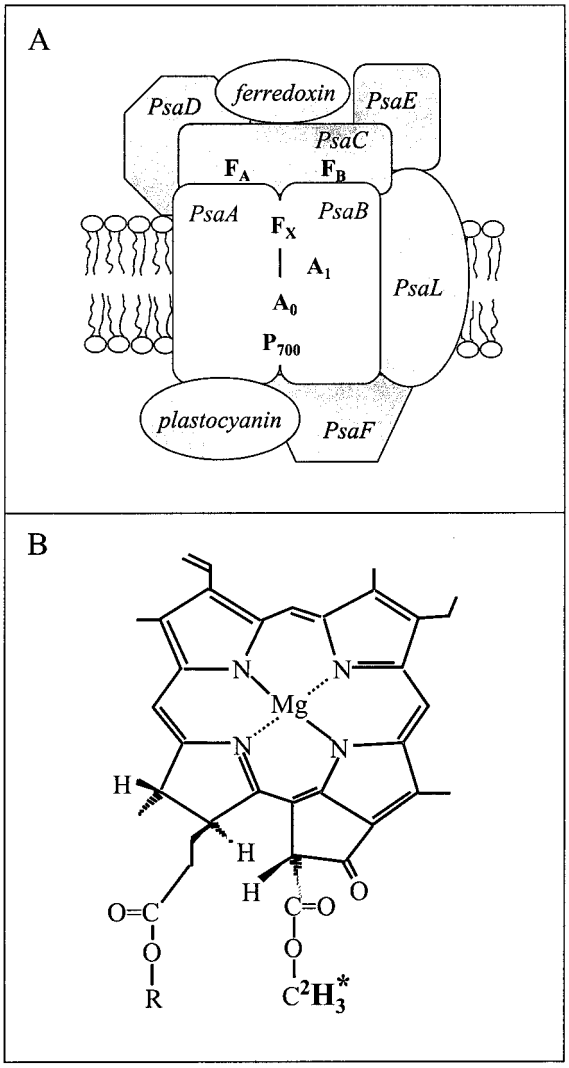

Figure 11. Cartoon model of the PSI structure, based on a reported structural model[120] (A), and deuteration of chlorophyll from methionine, according to the method previously described[34] (B).

isotopic labeling. This approach will identify chl bands shifted in frequency as a result of protein perturbations. In conjunction with amino acid labeling, these experiments will also identify any direct protein contributions to the difference spectrum. Such structural changes in the protein may be linked to the photooxidation reaction from a thermodynamic point of view and may contribute to the free energy of the oxidation reaction (see discussion of Figure 4). We began our studies investigating the oxidation of the primary donor, P700, in PSI. PSI (Figure 11A) carries out the light-driven oxidation of reduced plastocyanin and reduction of ferredoxin {see ref 116 for a review}. Electron transfer is initiated when P_{700} absorbs light. Subsequent electron-transfer reactions lead to production of a chl cation radical, P_{700}^+, and reduction of a chl acceptor molecule, A_0, a phylloquinone acceptor, A_1, and an intrinsic iron−sulfur cluster, F_x.[116−118] These components are bound to two subunits, psaA and psaB, that compose the heterodimeric core of PSI.[119] A 4 angstrom model of the PSI structure has been presented,[120] and a higher resolution structure is in progress {Prof. H. T. Witt, personal communication}.

In our reaction-induced FT-IR studies of PSI, we have performed an experiment in which the chl 13^3 methoxy was $^2H_3$-labeled (Figure 11B).[34] Deuteration of this methyl group will downshift vibrational modes arising from the ester group.

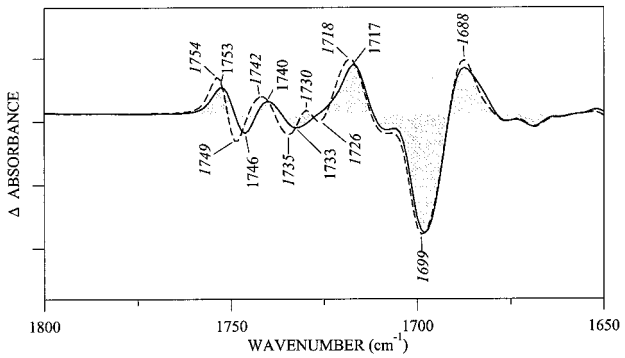

Figure 12. Light-minus-dark FT-IR spectrum associated with P_{700}^+-minus-P_{700} in PSI isolated from cyanobacteria grown on $^1H_3$-methionine (dotted line) and $^2H_3$-methionine (solid line). Spectral conditions are reported in ref 34.

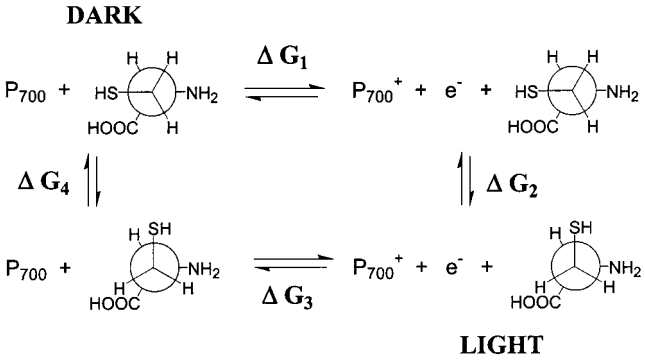

Figure 13. Speculative model showing a rotomer change at a cysteine residue and linkage to the photooxidation of P_{700} in PSI.

Upshifts of the ester C═O vibration are expected upon chl oxidation in vitro.[121] Therefore, ^{2}H-labeled samples should exhibit isotope shifts in the 1750−1720 cm^{-1} spectral region. As shown in Figure 12, such shifts were indeed observed. Because there is no significant deuterium incorporation into asparatic or glutamic acid residues,[35] vibrational contributions from chl ester groups were distinguished from amino acid residue contributions. The surprising result of this study was that multiple (four) C═O ester contributions to the spectrum were identified.[34] This number is more than can be accounted for by the dimeric nature of P_{700} and may indicate a static or dynamic heterogeneity in the structure of P_{700} and/or P_{700}^+. This result is still under investigation.

We have also detected a structural change in a cysteine residue that may be linked to the photooxidation of the primary donor.[36] The SH stretching vibration of protein cysteine residues occurs in a spectral region that contains no other fundamental vibrations.[122,123] This facilitates assignment of SH bands. The SH band observed in cyanobacterial PSI has a negative spectral feature at 2560 cm^{-1} and a positive band at 2551 cm^{-1}. On the basis of the literature,[122,123] the observed S−H band may arise from a hydrogen-bonded cysteine (S−H−X) that is perturbed by an increase in hydrogen bonding, by a change in rotomer conformation at the C−SH bond, or by the electric field generated by P_{700}^+. The observed temperature dependence of the vibrational bands favors the explanation that a change in rotomer conformation (Figure 13) is the perturbative element.[36] These cyanobacterial SH frequencies are identical to those previously observed for SH bands in heliobacterial reaction centers upon photooxidation of its primary donor, P_{798}.[19] This is of importance because heliobacterial reaction centers carry out anoxygenic photosynthesis but may be closely evolutionarily related to cyanobacterial PSI.[124−126] This observation suggests

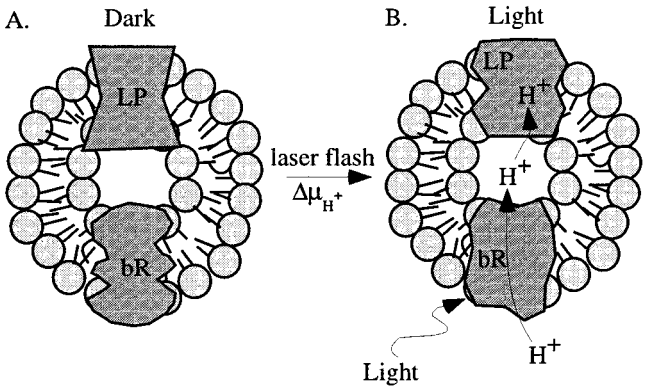

Figure 14. Reconstitution of lactose permease and bacteriorhodopsin and the effect of the light-triggered electrochemical gradient on the permease. This figure was graciously provided by Dr. J. Patzlaff.

that the S−H environment is similar and that the cysteine may play a similar functional role in the two reaction centers. These first efforts form a basis for investigating the impact of the protein environment on the energetics of chl oxidation in PSI and PSII.

Transport

In secondary active transport, an electrochemical gradient drives the accumulation of substrates inside the cell. The lactose permease is such a secondary active transporter {reviewed in ref 127}. The permease is a symporter that transports a proton and lactose with one-to-one stoichiometry.[128] The permease can catalyze several processes, including lactose transport against a lactose concentration gradient; this uphill lactose transport is driven by a H^+ gradient.[127] A minimum model for the linked transport of a proton and lactose postulates that there are at least two different conformational states of the permease, one in which the lactose and proton binding site are accessible from the outside and one in which the lactose and proton binding side are accessible from the inside.[129] In this model, the effect of the electrochemical potential is to cause conformational interconversion between these forms of the transporter. This is a minimum model, and the conformational transition may be much more complex. Both an electric potential and the proton gradient can drive uphill lactose transport.[127] Therefore, changes in the pK_a of ionizable residues are likely triggers for the conformational rearrangement.

We set out to see if reaction-induced FT-IR spectroscopy could be used to acquire direct information about the structural changes that take place in the permease. Because a single sample must be modulated between two functional states of interest to construct an accurate difference spectrum, bacteriorhodopsin was employed as a light-inducible trigger of an electrochemical gradient (Figure 14). Permease was purified and then reconstituted into liposomes.[130] Bacteriorhodopsin-containing purple membrane was isolated and fused with these liposomes by a freeze−thaw technique.[37] Control experiments on the co-reconstituted vesicles demonstrated a stimulation of lactose efflux under illumination and suggested that each permease-containing liposome also contained one or more bacteriorhodopsin molecules.[37] These experiments also showed that bacteriorhodopsin was preferentially oriented to pump protons into the liposome (Figure 14). This preferential orientation of the reconstituted form of bacteriorhodopsin has been observed previously.[131−133]

This reconstituted system is useful for reaction-induced FT-IR experiments, because a laser flash can be employed to trigger the reaction of interest, i.e., the imposition of a gradient (Figure 14). Experiments have been carried out in the presence and absence of lactose. In the absence of lactose, the permease cannot make a conformational switch between the inside and outside accessible forms.[129] However, it has been shown that the imposition of the gradient causes a decrease in the K_m for lactose by several orders of magnitude.[134] If measurements are conducted in the presence of lactose and on the time scale of the transport reactions, then the observable state would be any intermediate that builds up in concentration before a rate-limiting step in the mechanism.

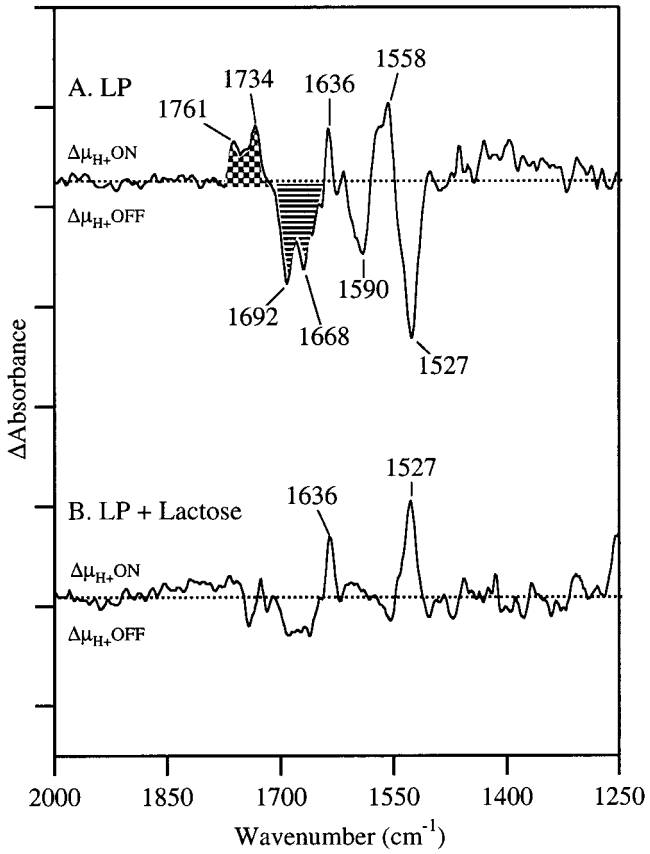

Figure 15. Reaction-induced FT-IR spectrum associated with the imposition of an electrochemical gradient on the lactose permease in the absence (A) and presence of lactose (B). Spectral conditions are reported in ref 37.

Figure 15A presents the difference FT-IR spectrum associated with the imposition of the electrochemical gradient in the absence of lactose. The bacteriorhodopsin contributions have been subtracted out using an optical measurement of the bacteriorhodopsin and total protein concentrations.[37] The lactose permease spectrum decays in the 5 min following saturating laser flashes (data not shown), presumably with the decay of a component of the proton motive force. A positive vibrational band attributable to the permease is observed at 1734 cm^{-1} (Figure 15A); this band is tentatively assigned to the C═O stretch of carboxylic acid residues in the permease.[37] This assignment is based on group frequency assignments and must be tested by isotopic labeling.

One interpretation of the spectrum shown in Figure 15A is that a pK_a or full protonation change occurs in carboxylic acid residues of the permease when the electrochemical gradient is applied. It is known that carboxylic acid residues at positions 126, 240, 269, and 325 modulate permease function {see refs 127 and 135 and references therein}; therefore the 1734 cm^{-1} band may originate from one of these amino acid residues.

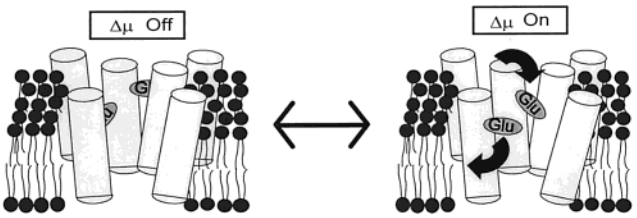

Figure 16. Speculative model showing the effects of the electrochemical potential on glutamic acid residues in the permease. This figure was graciously provided by Prof. R. J. Brooker.

Figure 16 shows a model summarizing speculative conclusions from these studies. In this model, imposition of a proton electrochemical gradient causes a dipole rearrangement in transmembrane α helices. Helix rearrangement leads to changes in the environment of one or more carboxylic acid side chains. Such structural changes could be involved in storage of free energy from the gradient.

In the presence of lactose, the permease spectrum is observed to change dramatically with a general decrease of amplitude throughout much of the 1800−1200 cm^{-1} region (Figure 15B). This is understandable if the lactose transport processes are fast on the time scale of the measurements performed. The turnover time for uphill transport is approximately 60 ms.[136] Our measurements have been conducted on the time scale of minutes,[37] so this is a reasonable hypothesis. Remaining spectral features, which are assignable to amide I and II vibrations (Figure 15B), may be consistent with a long-lived permease conformation, which differs in backbone hydrogen bonding from the original equilibrium structure. Future experiments will be performed in more rapid time regimes to follow conformational changes associated with transport in real time.

Summary

As assessed by hydrophobicity and by the presence of at least one predicted transmembrane helix in the primary sequence, membrane proteins may account for up to 40% of the proteins encoded in a eukaryotic genome {see for example refs 137 and 138}. However, less than 2% of X-ray and NMR protein structures are derived from membrane proteins. In addition to photosynthesis, respiration, and transport, membrane proteins are also involved in other important processes, including transmembrane signaling and regulation of cell growth and metabolism. Clearly, our understanding of biological chemistry is limited by our lack of knowledge concerning the structure, function, and folding of membrane proteins, and new approaches to understanding structure and function in membrane-associated enzymes are crucial.

FT-IR spectroscopy is such a valuable approach. Reaction-induced FT-IR spectroscopy has been employed in order to provide mechanistic and dynamic information concerning many light-activatable enzymes. One strength of the technique is its ability to obtain information about the structure of components in situ, thus illustrating how the protein environment alters the function of amino acid side chains and prosthetic groups. Derivation of a complete structural picture is possible when specific isotopic labeling and normal coordinate analysis can be applied. A second strength of reaction-induced FT-IR spectroscopy is its ability to identify all the structural alterations, which are linked to and caused by a functional perturbation. These linked alterations can be critical in the thermodynamic and kinetic control of enzymatic function. The recent extension of reaction-induced FT-IR techniques to a transport protein, that is not directly light-activatable, means that FT-IR spectroscopy will be a more widely applicable and more easily implemented technique in the years ahead.

Acknowledgment. We thank Prof. G. MacDonald, Dr. K. Bixby, Dr. M. Bernard, Dr. J. Steenhuis, Dr. Q. Yan, Dr. M. R. Razeghifard, Prof. J. Liang, Prof. R. Hutchison, Prof. R. Sachs, Dr. J. Patzlaff, Ms. I. Ayala, Dr. B. Svensson, and Mr. K. Halverson for their experimental and intellectual contributions to the work described here. For many helpful conversations, we are also grateful to Dr. R. Boerner, Mr. G. Noren, Dr. C. Ma, Mr. A. Ouellette, Dr. Y. Zhou, Dr. J. Larson, Dr. C. Sacksteder, Dr. L. Anderson, Dr. M. Maderia, and Prof. C. Woodward. For assistance in the preparation of this manuscript and its figures, the authors thank Dr. K. Bixby, Dr. J. Patzlaff, and Prof. R. Brooker. Finally, B.A.B. thanks her collaborators in the work described here: Profs. R. Brooker (University of Minnesota), R. Wheeler (University of Oklahoma), and C. F. Yocum (University of Michigan). The authors also acknowledge mass spectrometry assistance from the Mass Spectrometry Consortium for the Life Sciences and from Mr. T. Krick. Supported by NIH GM43273 (B.A.B.), NSF 98-08934 (B.A.B.), and NIH GM53259 (R. J. Brooker/B.A.B).

References and Notes

(1) Kim, S.; Liang, J.; Barry, B. A. *Proc. Natl. Acad. Sci. U.S.A.* **1997**, *94*, 14406−14412.
(2) MacDonald, G. M.; Bixby, K. A.; Barry, B. A. *Proc. Natl. Acad. Sci. U.S.A.* **1993**, *90*, 11024−11028.
(3) Rothschild, K. J.; Zagaeski, M.; Cantore, W. A. *Biochem. Biophys. Res. Commun.* **1981**, *103*, 483−489.
(4) Bagley, K.; Dollinger, G.; Eisenstein, L.; Singh, A. K.; Zimanyi, L. *Proc. Natl. Acad. Sci. U.S.A.* **1982**, *79*, 4972−4976.
(5) Stoeckenius, W.; Bogomolni, R. A. *Annu. Rev. Biochem.* **1982**, *52*, 587−616.
(6) Braiman, M.; Mathies, R. *Biochemistry* **1980**, *19*, 5421−5428.
(7) Pande, J.; H.Callender, R.; Ebrey, T. G. *Proc. Natl. Acad. Sci. U.S.A.* **1981**, *78*, 7379−7382.
(8) Braiman, M.; Mathies, R. *Proc. Natl. Acad. Sci. U.S.A.* **1982**, *79*, 403−407.
(9) Luecke, H.; Schobert, B.; Richter, H.-T.; Cartailler, J.-P.; Lanyi, J. K. *Science* **1999**, *286*, 255−260.
(10) Royant, A.; Edman, K.; Urshy, T.; Pebay-Peyroula, E.; Landau, E. M.; Neutze, R. *Science* **2000**, *406*, 645 648.
(11) Sass, H. J.; Buldt, G.; Gessinich, R.; Hehn, D.; Neff, D.; Schlesinger, R.; Berendzen, J.; Ormos, P. *Science* **2000**, *406*, 649−653.
(12) Subranmaniam, S.; Henderson, R. *Science* **2000**, *406*, 653−657.
(13) Rothschild, K. J. *J. Bioenerg. Biomembr.* **1992**, *24*, 147−167.
(14) Rath, P.; Olson, K. D.; Spudich, J. L.; Rothschild, K. J. *Biochemistry* **1994**, *33*, 5600−5606.
(15) Braiman, M. S.; Walter, T. J.; Briarcheck, D. M. *Biochemistry* **1994**, *33*, 1629−1635.
(16) Maeda, A.; Ohkita, Y. J.; Sasaki, J.; Shichida, Y.; Yoshizawa, T. *Biochemistry* **1993**, *32*, 12033−12038.
(17) Foerstendorf, H.; Mummert, E.; Schafer, E.; Scheer, H.; Siebert, F. *Biochemistry* **1996**, *35*, 10793−10799.
(18) Breton, J.; Boullais, C.; Berger, G.; Mioskowski, C.; Nabedryk, E. *Biochemistry* **1995**, *34*, 11606−11616.
(19) Noguchi, T.; Fukami, Y.; Oh-oka, H.; Inoue, Y. *Biochemistry* **1997**, *36*, 12329−12336.
(20) Behr, J.; Hellwig, P.; Mäntele, W.; Michel, H. *Biochemistry* **1998**, *37*, 7400−7406.
(21) MacDonald, G. M.; Barry, B. A. *Biochemistry* **1992**, *31*, 9848−9856.
(22) Bernard, M. T.; MacDonald, G. M.; Nguyen, A. P.; Debus, R. J.; Barry, B. A. *J. Biol. Chem.* **1995**, *270*, 1589−1594.
(23) MacDonald, G. M.; Steenhuis, J. J.; Barry, B. A. *J. Biol. Chem.* **1995**, *270*, 8420−8428.
(24) Steenhuis, J. J.; Barry, B. A. *J. Am. Chem. Soc.* **1996**, *118*, 11927−11932.
(25) Steenhuis, J. J.; Barry, B. A. *J. Phys. Chem. B* **1997**, *101*, 6652−6660.
(26) Kim, S.; Ayala, I.; Steenhuis, J. J.; Gonzalez, E. T.; Razeghifard, M. R.; Barry, B. A. *Biochim. Biophys. Acta* **1998**, *1366*, 330−354.
(27) Kim, S.; Barry, B. A. *Biochemistry* **1998**, *37*, 13882−13892.
(28) Kim, S.; Barry, B. A. *Biophys. J.* **1998**, *74*, 2588−2600.
(29) Steenhuis, J. J.; Barry, B. A. *J. Phys. Chem. B* **1998**, *102*, 4−8.

(30) Ayala, I.; Kim, S.; Barry, B. A. *Biophys. J.* **1999**, *77*, 2137−2144.
(31) Hutchison, R. S.; Steenhuis, J. J.; Yocum, C. F.; Razeghifard, R. M.; Barry, B. A. *J. Biol. Chem.* **1999**, *274*, 31987−31995.
(32) Razeghifard, M. R.; Kim, S.; Patzlaff, J. S.; Hutchison, R. S.; Krick, T.; Ayala, I.; Steenhuis, J. J.; Boesch, S. E.; Wheeler, R. A.; Barry, B. A. *J. Phys. Chem. B* **1999**, *103*, 9790−9800.
(33) Steenhuis, J. J.; Hutchison, R. S.; Barry, B. A. *J. Biol. Chem.* **1999**, *274*, 14609−14616.
(34) Kim, S.; Barry, B. A. *J. Am. Chem. Soc.* **2000**, *122*, 4980−4981.
(35) Kim, S.; Patzlaff, J.; Krick, T.; Ayala, I.; Sachs, R. K.; Barry, B. A. *J. Phys. Chem. B* **2000**, *104*, 9720−9727.
(36) Kim, S.; Barry, B. A. Submitted.
(37) Patzlaff, J. S.; Brooker, R. J.; Barry, B. A. *J. Biol. Chem.* **2000**, *275*, 28695−28700.
(38) Britt, R. D. In *Oxygenic Photosynthesis: The Light Reactions*; Ort, D. R., Yocum, C. F., Eds.; Kluwer Academic Publisher: Dordrecht, The Netherlands, 1996; Vol. 4, pp 137−164.
(39) Barry, B. A. *Methods Enzymol.* **1995**, *258*, 303−319.
(40) Boerner, R. J.; Barry, B. A. *J. Biol. Chem.* **1993**, *268*, 17151−17154.
(41) Gerken, S.; Brettel, K.; Schlodder, E.; Witt, H. T. *FEBS Lett.* **1988**, *237*, 69−75.
(42) Barry, B. A.; Babcock, G. T. *Proc. Natl. Acad. Sci. U.S.A.* **1987**, *84*, 7099−7103.
(43) Joliot, P.; Kok, B. In *Bioenergetics of Photosynthesis*; Govindjee, Ed.; Academic Press: New York, 1975; pp 388−412.
(44) Bricker, T.; Frankel, L. *Photosynth. Res.* **1998**, *56*, 157−173.
(45) Deisenhofer, J.; Michel, H. *Science* **1989**, *245*, 1463−1473.
(46) Okamura, M. Y.; Isaacson, R. A.; Feher, G. *Proc. Natl. Acad. Sci. U.S.A.* **1975**, *72*, 3491−3495.
(47) Zhao, X.; Ogura, T.; Okamura, M.; Kitagawa, T. *J. Am. Chem. Soc.* **1997**, *119*, 5263−5264.
(48) Berthomieu, C.; Nabedryk, E.; Mäntele, W.; Breton, J. *FEBS Lett.* **1990**, *269*, 363−367.
(49) Zhang, H.; Razeghifard, M. R.; Fischer, G.; Wydrzynski, T. *Biochemistry* **1997**, *36*, 11762−11768.
(50) Koulougliotis, D.; Tang, X.-S.; Diner, B. A.; Brudvig, G. W. *Biochemistry* **1995**, *34*, 2850−2856.
(51) Debus, R. J.; Barry, B. A.; Babcock, G. T.; McIntosh, L. *Proc. Natl. Acad. Sci. U.S.A.* **1988**, *85*, 427−430.
(52) Debus, R. J.; Barry, B. A.; Sithole, I.; Babcock, G. T.; McIntosh, L. *Biochemistry* **1988**, *27*, 9071−9074.
(53) Vermaas, W. F. J.; Rutherford, A. W.; Hansson, Ö. *Proc. Natl. Acad. Sci. U.S.A.* **1988**, *85*, 8477−8481.
(54) Metz, J. G.; Nixon, P. J.; Rögner, M.; Brudvig, G. W.; Diner, B. A. *Biochemistry* **1989**, *28*, 6960−6969.
(55) Noren, G. H.; Barry, B. A. *Biochemistry* **1992**, *31*, 3335−3342.
(56) Noren, G. H.; Boerner, R. J.; Barry, B. A. *Biochemistry* **1991**, *30*, 3943−3950.
(57) Boerner, R. J.; Bixby, K. A.; Nguyen, A. P.; Noren, G. H.; Debus, R. J.; Barry, B. A. *J. Biol. Chem.* **1993**, *268*, 1817−1823.
(58) Styring, S.; Rutherford, A. W. *Biochemistry* **1987**, *26*, 2401−2405.
(59) Razeghifard, M. R.; Klughammer, C.; Pace, R. J. *Biochemistry* **1997**, *36*, 86−92.
(60) Babcock, G. T.; Sauer, K. *Biochim. Biophys. Acta* **1973**, *325*, 504−519.
(61) Boussac, A.; Etienne, A. L. *Biochim. Biophys. Acta* **1984**, *766*, 576−581.
(62) Marcus, R. A. *Pure Appl. Chem.* **1997**, *69*, 13−29.
(63) Tommos, C.; Davidsson, L.; Svensson, B.; Madsen, C.; Vermaas, W.; Styring, S. *Biochemistry* **1993**, *32*, 5436−5441.
(64) Campbell, K. A.; Peloquin, J. M.; Diner, B. A.; Tang, X.-S.; Chisholm, D. A.; Britt, R. D. *J. Am. Chem. Soc.* **1997**, *119*, 4787−4788.
(65) Hays, A.-M. A.; Vassiliev, I. R.; Golbeck, J. H.; Debus, R. J. *Biochemistry* **1998**, *37*, 11352−11365.
(66) Mamedov, F.; Sayre, R. T.; Styring, S. *Biochemistry* **1998**, *37*, 14245−14256.
(67) Roffey, R. A.; van Wijk, K.-J.; Sayre, R. T.; Styring, S. *J. Biol. Chem.* **1994**, *269*, 5115−5121.
(68) Hays, A. M. A.; Vassiliev, I. R.; Golbeck, J. H.; Debus, R. J. *Biochemistry* **1999**, *38*, 11851−11865.
(69) Force, D. A.; Randall, D. W.; Britt, R. D.; Tang, X.-S.; Diner, B. A. *J. Am. Chem. Soc.* **1995**, *117*, 12643−12644.
(70) Diner, B. A.; Force, D. A.; Randall, D. W.; Britt, R. D. *Biochemistry* **1998**, *37*, 17931−17943.
(71) Tu, C.; Silverman, D. N. *Biochemistry* **1989**, *28*, 7913−7918.
(72) Barrick, D. *Biochemistry* **1994**, *33*, 6546−6554.
(73) Fitzgerald, M. N.; Churchill, M. J.; McRee, D. E.; Goodin, D. B. *Biochemistry* **1994**, *33*, 3807−3818.
(74) Decatur, S. M.; Boxer, S. G. *Biochemistry* **1995**, *34*, 2122−2129.
(75) Wilks, A.; Sun, J.; Loehr, T. M.; Ortiz de Montellano, P. R. *J. Am. Chem. Soc.* **1995**, *117*, 2925−2926.
(76) Goldsmith, J. O.; King, B.; Boxer, S. G. *Biochemistry* **1996**, *35*, 2421−2428.
(77) Alternate assignments of the $D^{\bullet}$ and $Z^{\bullet}$ ν(CO) vibrations have been reported. The $D^{\bullet}$ CO stretching vibration was assigned to a band at 1503/1504 cm^{-1};[78] the $Z^{\bullet}$ CO stretching vibration was assigned to a band at 1512 cm^{-1}.[79] However, that $D^{\bullet}$ result has been shown to be dependent on and caused by the presence of formate/phosphate in sample buffers, which change PSII secondary structure, accelerate the decay kinetics of $D^{\bullet}$, and shift the vibrational modes of $D^{\bullet}$.[27] In our view, that $Z^{\bullet}$ result is a misassignment based on the use of time regimes where $Z^{\bullet}$ decay is essentially complete.[30] The 1512 cm^{-1} band may be attributable to a neutral tyrosine residue.[30]
(78) Hienerwadel, R.; Boussac, A.; Breton, J.; Diner, B. A.; Berthomieu, C. *Biochemistry* **1997**, *36*, 14712−14723. Noguchi, T.; Inoue, Y.; Tang, X.-S. *Biochemistry* **1997**, *36*, 14705−14711.
(79) Berthomieu, C.; Hienerwadel, R.; Boussac, A.; Breton, J.; Diner, B. A. *Biochemistry* **1998**, *37*, 10547−10554.
(80) Garfinkel, D.; Edsall, J. T. *J. Am. Chem. Soc.* **1958**, *80*, 3807−3812.
(81) Columbo, L.; Bleckmann, P.; Schrader, B.; Scheider, R.; Plesser, T. *J. Chem. Phys.* **1974**, *61*, 3270−3278.
(82) Wolff, H.; Muller, H. *J. Chem. Phys.* **1974**, *60*, 2938−2939.
(83) Caswell, D. S.; Spiro, T. G. *J. Am. Chem. Soc.* **1986**, *108*, 6470−6477.
(84) Majoube, M.; Vergoten, G. *J. Mol. Struct.* **1992**, *266*, 345−352.
(85) Harhay, G. P.; Hudson, B. S. *J. Phys. Chem.* **1993**, *97*, 8158−8164.
(86) Markham, L. M.; Mayne, L. C.; Hudson, B. S.; Zgierski, M. Z. *J. Phys. Chem.* **1993**, *97*, 10319−10325.
(87) Noguchi, T.; Ono, T.-A.; Inoue, Y. *Biochemistry* **1992**, *31*, 5953−5956.
(88) Zhang, H.; Fischer, G.; Wydrzynski, T. *Biochemistry* **1998**, *37*, 5511−5517.
(89) Chu, H. A.; Gardner, M. T.; O'Brien, J. P.; Babcock, G. T. *Biochemistry* **1999**, *38*, 4533−4541.
(90) Barry, B. A. *Photosynth. Res.* **2000**, *65*, 197−198.
(91) Nanba, O.; Satoh, K. *Proc. Natl. Acad. Sci. U.S.A.* **1987**, *84*, 109−112.
(92) Zouni, A.; Witt, H. T.; Kern, J.; Fromme, P.; Krauss, N.; Saenger, W.; Orth, P. *Nature* **2001**, *409*, 739−743.
(93) Trebst, A. *Z. Naturforsch.* **1986**, *41c*, 240−245.
(94) Barry, B. A.; Boerner, R. J.; de Paula, J. C. In *The Molecular Biology of the Cyanobacteria*; D. Bryant, Ed.; Kluwer Academic Publishers: Dordrecht, 1994; Vol. 1, pp 215−257.
(95) Boerner, R. J.; Nguyen, A. P.; Barry, B. A.; Debus, R. J. *Biochemistry* **1992**, *31*, 6660−6672.
(96) Nixon, P. J.; Diner, B. A. *Biochemistry* **1992**, *31*, 942−948.
(97) Nordlund, P.; Sjöberg, B.-M.; Eklund, H. *Nature* **1990**, *345*, 593−598.
(98) Rosenzweig, A. C.; Frederick, C. A.; Lippard, S. J.; Nordlund, P. *Nature* **1993**, *366*, 537−543.
(99) Hutchison, R. S.; Betts, S. D.; Yocum, C. F.; Barry, B. A. *Biochemistry* **1998**, *37*, 5643−5653.
(100) Äkerlund, H.-E.; Jansson, C. *FEBS Lett.* **1981**, *124*, 229−232.
(101) Yamomoto, Y.; Doi, M.; Tamura, N.; Nishimura, N. *FEBS Lett.* **1981**, *133*, 265−268.
(102) Ono, T.; Inoue, Y. *FEBS Lett.* **1983**, *164*, 252−260.
(103) Miyao, M.; Murata, N. *FEBS Lett.* **1984**, *170*, 350−354.
(104) Bricker, T. M. *Biochemistry* **1992**, *31*, 4623−4628.
(105) Surewicz, W. K.; Mantsch, H. A.; Chapman, D. *Biochemistry* **1993**, *32*, 389−394.
(106) Jackson, M.; Mantsch, H. H. *Crit. Rev. Biochem. Mol. Biol.* **1995**, *30*, 95−120.
(107) Byler, D. M.; Susi, H. *Biopolymers* **1986**, *25*, 469−487.
(108) Krimm, S.; Bandekar, J. In *Advances in Protein Chemistry*; Anfinsen, C. B., Edsall, J. T., Richards, F. M., Eds.; Academic Press: New York, 1986; Vol. 38, pp 181−364.
(109) Ahmed, A.; Tajmir-Riahi, H. A.; Carpentier, R. *FEBS Lett.* **1995**, *363*, 65−68.
(110) Lydakis-Simantiris, N.; Hutchison, R. S.; Betts, S. D.; Barry, B. A.; Yocum, C. F. *Biochemistry* **1999**, *38*, 404−414.
(111) Miyao, M.; Murata, N.; Lavorel, J.; Maison-Peteri, B.; Boussac, A.; Etienne, A.-L. *Biochim. Biophys. Acta* **1987**, *890*, 151−159.
(112) Vass, I.; Ono, T.; Inoue, Y. *Biochim. Biophys. Acta* **1987**, *892*, 224−235.
(113) Burnap, R. L.; Shen, J.-R.; Jursinic, P. A.; Inoue, Y.; Sherman, L. A. *Biochemistry* **1992**, *31*, 7404−7410.
(114) van Gorkom, H. J.; Schelvis, J. P. M. *Photosynth. Res.* **1993**, *38*, 297−301.
(115) Matysik, J.; Alia; Gast, P.; van Gorkom, H. J.; Hoff, A. J.; de Groot, H. J. M. *Proc. Natl. Acad. Sci. U.S.A.* **2000**, *97*, 9865−9870.
(116) Brettel, K. *Biochim. Biophys. Acta* **1997**, *1318*, 322−373.

(117) Setif, P. In *The Photosystems: Structure, Function and Molecular Biology*; Barber, J., Ed.; Elsevier: The Hague, 1992; pp 471−499.

(118) Golbeck, J. H. In *The Molecular Biology of Cyanobacteria*; Bryant, D. A., Ed.; Kluwer Academic Publishers: The Netherlands, 1994; pp 319−360.

(119) Bryant, D. A. In *The Photosystems: Structure, Function and Molecular Biology*; Barber, J., Ed.; Elsevier: Amsterdam, 1992; Vol. 11, pp 501−549.

(120) Krauss, N.; Schubert, W. D.; Klukas, O.; Fromme, P.; Witt, H. T.; Saenger, W. *Nat. Struct. Biol.* **1996**, *3*, 965−973.

(121) Nabedryk, E.; Leonhard, M.; Mäntele, W.; Breton, J. *Biochemistry* **1990**, *29*, 3242−3247.

(122) Li, H.; G. J. Thomas, J. *J. Am. Chem. Soc.* **1991**, *113*, 456−462.

(123) Li, H.; Wurrey, C. J.; G. J. Thomas, J. *J. Am. Chem. Soc.* **1992**, *114*, 7463−7469.

(124) Liebl, U.; Mochensturm-Wilson, M.; Trost, J. T.; Brune, D. C.; Blankenship, R.; Vermaas, W. *Proc. Natl. Acad. Sci. U.S.A.* **1993**, *90*, 7124−7128.

(125) Xiong, J.; Inoue, K.; Bauer, C. E. *Proc. Natl. Acad. Sci. U.S.A.* **1998**, *95*, 14851−14856.

(126) Xiong, J.; Fischer, W. M.; Inoue, K.; Nakahara, M.; Bauer, C. E. *Science* **2000**, *289*, 1724−1730.

(127) Kaback, H. R.; Wu, J. *Acc. Chem. Res.* **1999**, *32*, 805−813.

(128) West, I. C.; Mitchell, P. *Biochem. J.* **1973**, *132*, 587−592.

(129) Winkler, H. H.; Wilson, T. H. *J. Biol. Chem.* **1966**, *241*, 2200−2211.

(130) Patzlaff, J. S.; Moeller, J. A.; Barry, B. A.; Brooker, R. J. *Biochemistry* **1998**, *37*, 15363−15375.

(131) Racker, E.; Stoeckenuis, W. *J. Biol. Chem.* **1974**, *249*, 662−663.

(132) Lozier, R. H.; Niederberger, W.; Bogomolni, R. A.; Hwang, S.-B.; Stoeckenius, W. *Biochim. Biophys. Acta* **1976**, *440*, 545−556.

(133) Gerber, G. E.; Gray, C. P.; Wildenauer, D.; Khorana, H. G. *Proc. Natl. Acad. Sci. U.S.A.* **1977**, *74*, 5426−5430.

(134) Kaczorowski, G. J.; Robertson, D. E.; Kaback, H. R. *Biochemistry* **1979**, *18*, 3697−3704.

(135) Johnson, J. L.; Brooker, R. J. *J. Biol. Chem.* **1999**, *274*, 4074−4081.

(136) Kaback, H. R. *Annu. Rev. Biophys. Biophys. Chem.* **1986**, *15*, 279−319.

(137) Jacq, C.; Alt-Morbe, J.; Andre, B.; Arnold, W.; Bahr, A.; Ballesta, J.; Bargues, M.; Baron, L.; Becker, A.; Biteau, N.; Blocker, H.; Blugeon, C.; Boskovic, J.; Brandt, P.; Bruckner, M.; Buitrago, M.; Coster, F.; Delaveau, T.; del Rey, F.; Dujon, B.; Eide, L.; Garcia-Cantalejo, J.; Goffeau, A.; Gomez-Peris, A.; et al. *Nature* **1997**, *387* (6632 Suppl.), 75−78.

(138) Tettelin, H.; Agostoni Carbone, M.; Albermann, K.; Albers, M.; Arroyo, J.; Backes, U.; Barreiros, T.; Bertani, I.; Bjourson, A.; Bruckner, M.; Bruschi, C.; Carignani, G.; Castagnoli, L.; Cerdan, E.; Clemente, M.; Coblenz, A.; Coglievina, M.; Coissac, E.; Defoor, E.; Del Bino, S.; Delius, H.; Delneri, D.; de Wergifosse, P.; Dujon, B.; et al. *Nature* **1997**, *387* (6632 Suppl.), 81−84.